Supporting Information for "How well do regional climate models simulate the spatial dependence of precipitation? An application of pair-copula constructions"

DOI: 10.1002/

Ingrid Hobæk Haff,[1] Arnoldo Frigessi,[1,2] and Douglas Maraun[3]

Contents of this file

1. Figures S1 to S30

2. Tables S1 to S2

Introduction

This supplementary section includes additional tables and figures. Tables S1 and S2 show the percentage of each copula chosen for the observations and RCMs the full PCC for winter and summer, respectively. Figure S1 displays simulations from four bivariate

---

Corresponding author: I. Hobæk Haff, Statistics for Innovation, Norwegian Computing Center, PB 114 Blindern, NO-0373 Oslo, Norway. (ingrid@nr.no)

[1]Statistics for Innovation, Norwegian Computing Center, PB 114 Blindern, NO-0373 Oslo, Norway

[2]Oslo Centre for Biostatistics and Epidemiology, Department of Biostatistics, University of Oslo, PB 1122 Blindern, NO-0317 Oslo, Norway

[3]Ocean Circulation and Climate Dynamics, GEOMAR Helmholtz Centre for Ocean Research Kiel, Düsterbrooker Weg 20, 24105 Kiel, Germany

copulas. Further, Figures S17 and S18 are equivalent to Figures 10 and 11 in the paper, but instead of using the observed margins and RCM dependence, we have used RCM margins and observed dependence. Furthermore, all the figures that are shown only for the observations, METNO-HIRHAM and C4IRCA3 in the paper are displayed in this section for the remaning RCMs. After that, Figures S25 to S28 show 95% quantiles of daily precipitation in each grid box from the winter and summer seasons for the observations and each of the RCMs. Finally, Figures S29 and S30 display Spearman's ρ and the tail dependence between two cells for the winter and summer seasons for the observations, METNO-HIRHAM and DMI-HIRHAM5.

	Indep.	Gaussian	Stud. t	Clayton	Gumbel
Observations	49.2	16.2	26.1	3.1	5.4
METNO-HIRHAM	25	21.9	42.9	3.2	7.1
C4IRCA3	26.1	16.1	47.3	3.7	6.7
DMI-HIRHAM5	29.9	18.7	37.7	3.4	10.3
ETHZ-CLM	27.9	20.6	38.9	4.4	8.1
KNMI-RACMO2	31.1	18	40.4	2.4	8.1
METO-HC_HadRM3Q0	43.3	16.9	26.9	3.8	9.2
METO-HC_HadRM3Q16	41	18.4	27.9	3.9	8.8
METO-HC_HadRM3Q3	32	18.4	35.2	4.6	9.9
MPI-M-REMO	31.2	15.5	43.1	3.9	6.4
RPN_GEMLAM	45.2	11.6	39.1	2.5	1.6
SMHIRCA	44.2	6	46	2.3	1.5

Table S1. Percentage of copulas of each family chosen for the observations and the RCMs for winter.

	Indep.	Gaussian	Stud. t	Clayton	Gumbel
Observations	51.2	13.4	25.1	4.8	5.4
METNO-HIRHAM	30.5	15.7	44	3.9	5.9
C4IRCA3	29.8	16.9	43.4	4.7	5.3
DMI-HIRHAM5	30	20	39.2	3.2	7.6
ETHZ-CLM	30	17	41.7	4.1	7.1
KNMI-RACMO2	48.5	7.3	36.8	2.6	4.8
METO-HC_HadRM3Q0	43.1	13.8	30.7	3.7	8.8
METO-HC_HadRM3Q16	45.8	12.6	29.2	3.5	8.9
METO-HC_HadRM3Q3	42.7	11.4	33.9	3.9	8.1
MPI-M-REMO	44.4	6.4	41.7	3.1	4.4
RPN_GEMLAM	57	6.5	32.8	2.3	1.3
SMHIRCA	40.4	11.8	42.2	3.9	1.7

Table S2. Same as Table S1, but for summer.

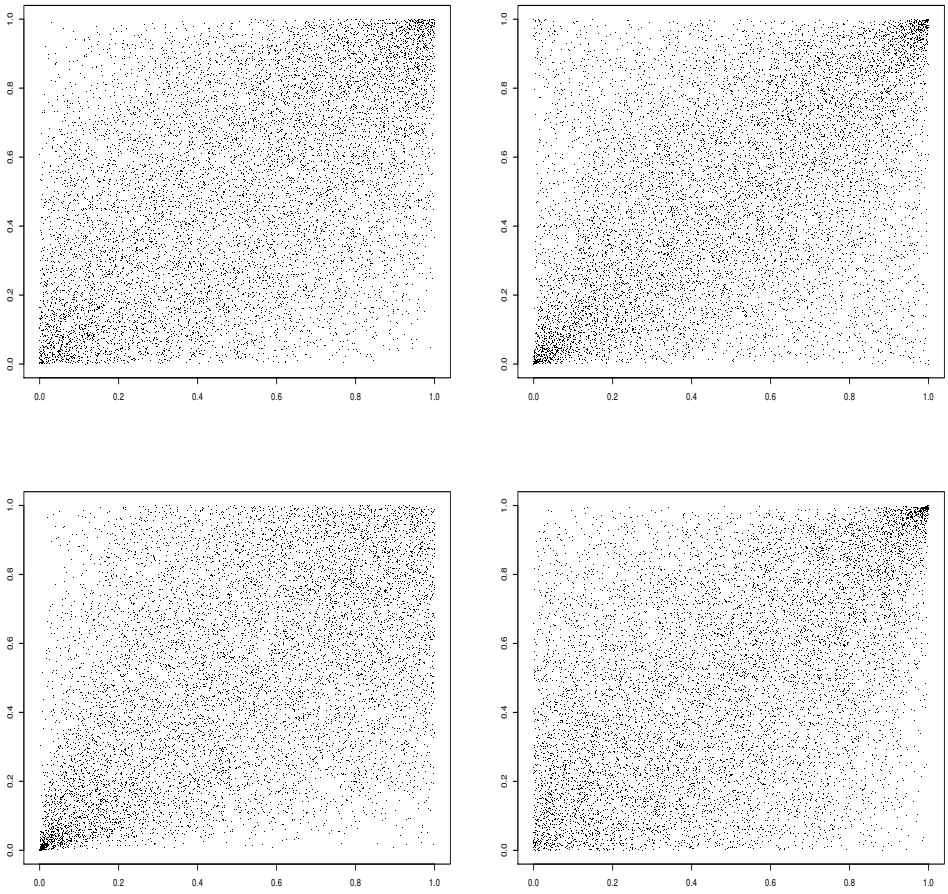

Figure S1. Simulations from four different bivariate copulas.

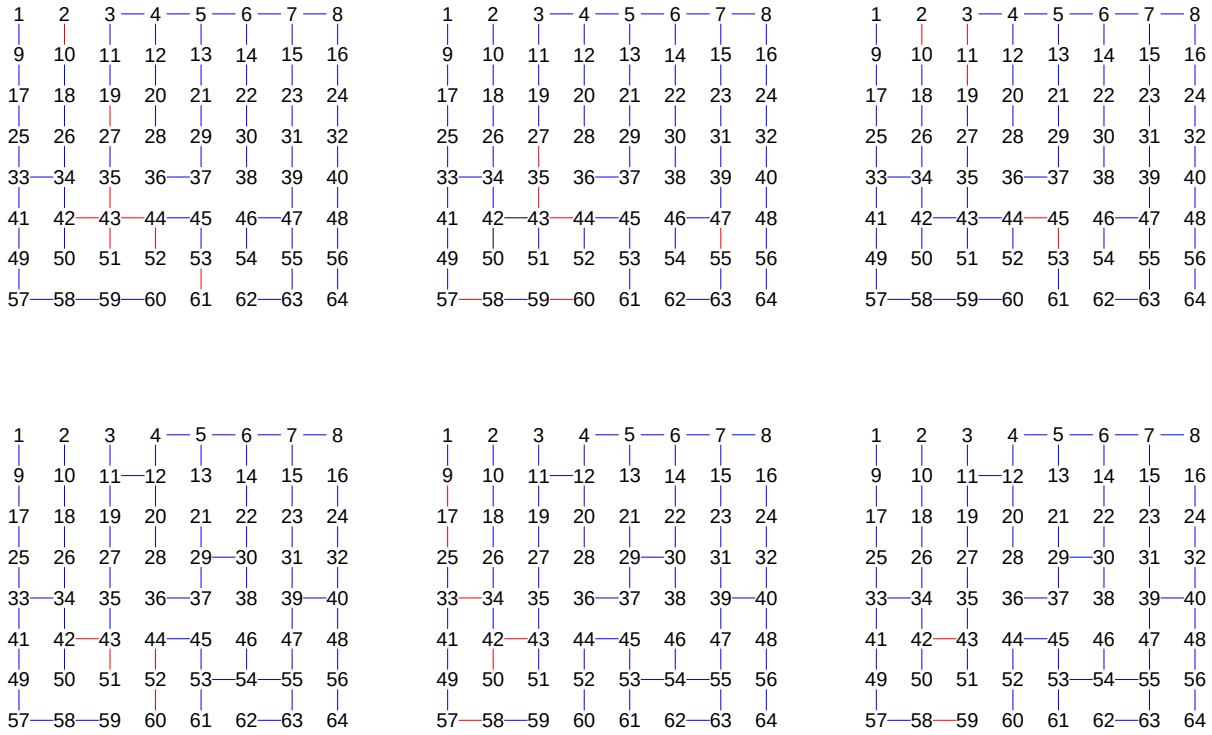

Figure S2. Ground level pairs selected for DMI-HIRHAM5 (left), ETHZ-CLM (centre) and KNMI-RACMO2 (right) from the winter (top) and summer (bottom) seasons. The colour of the lines represents the corresponding copula family (red=Student's t, blue=Gumbel, black=Gaussian, green=Clayton; note that the Clayton copula is never chosen on the ground level.

)

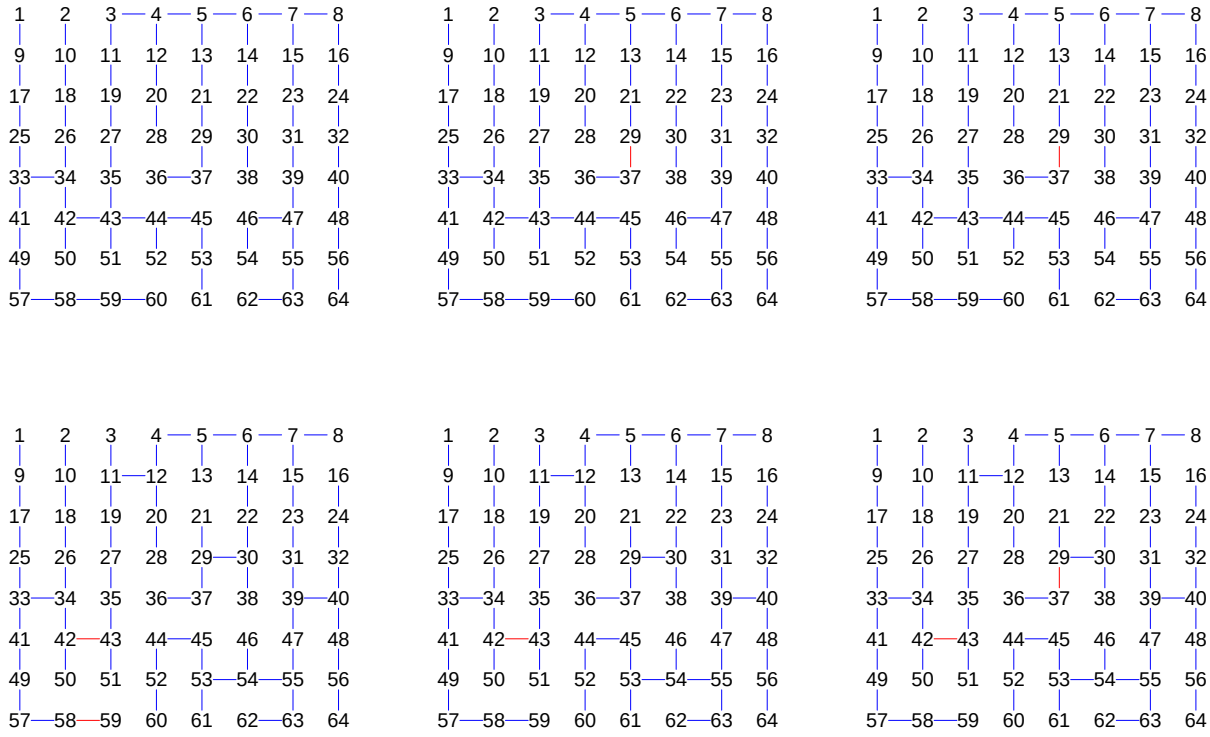

Figure S3. Ground level pairs selected for METO-HC_HadRM3Q0 (left), METO-HC_HadRM3Q16 (centre) and METO-HC_HadRM3Q3 (right) from the winter (top) and summer (bottom) seasons. The colour of the lines represents the corresponding copula family (red=Student's t, blue=Gumbel, black=Gaussian, green=Clayton; note that the Clayton copula is never chosen on the ground level.

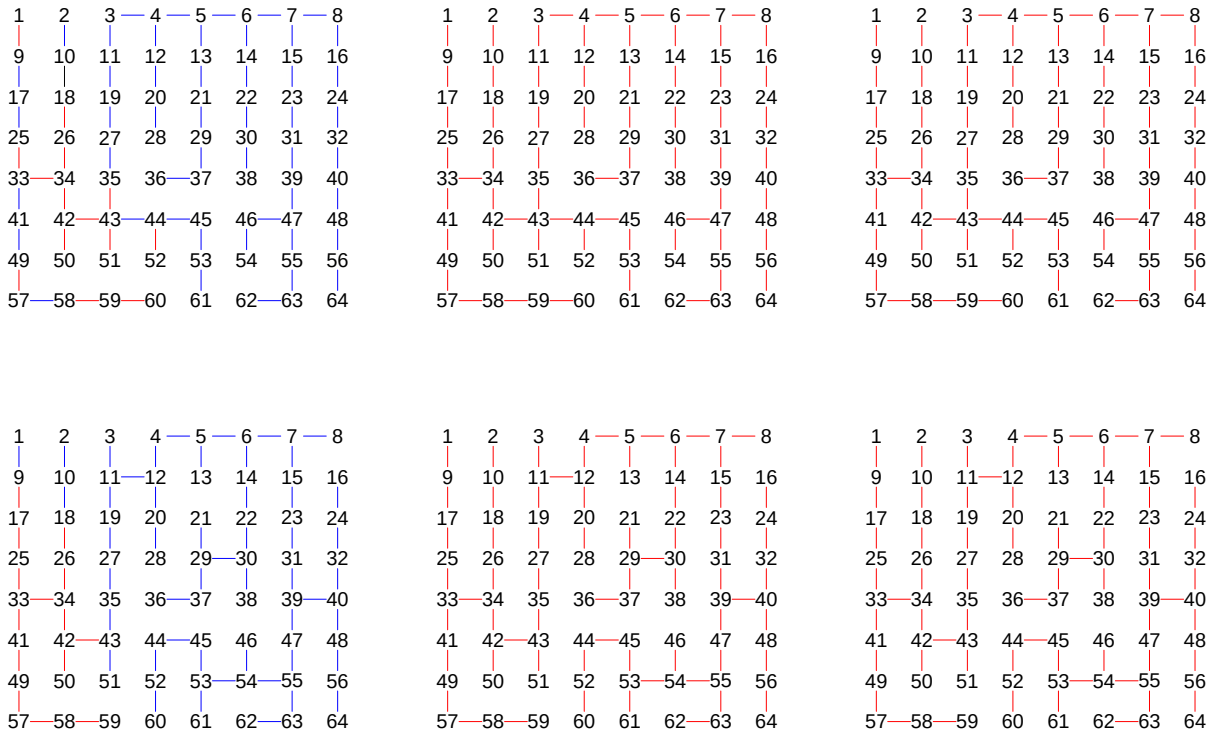

Figure S4. Ground level pairs selected for MPI-M-REMO (left), RPN_GEMLAM (centre) and SMHIRCA (right) from the winter (top) and summer (bottom) seasons. The colour of the lines represents the corresponding copula family (red=Student's t, blue=Gumbel, black=Gaussian, green=Clayton; note that the Clayton copula is never chosen on the ground level.

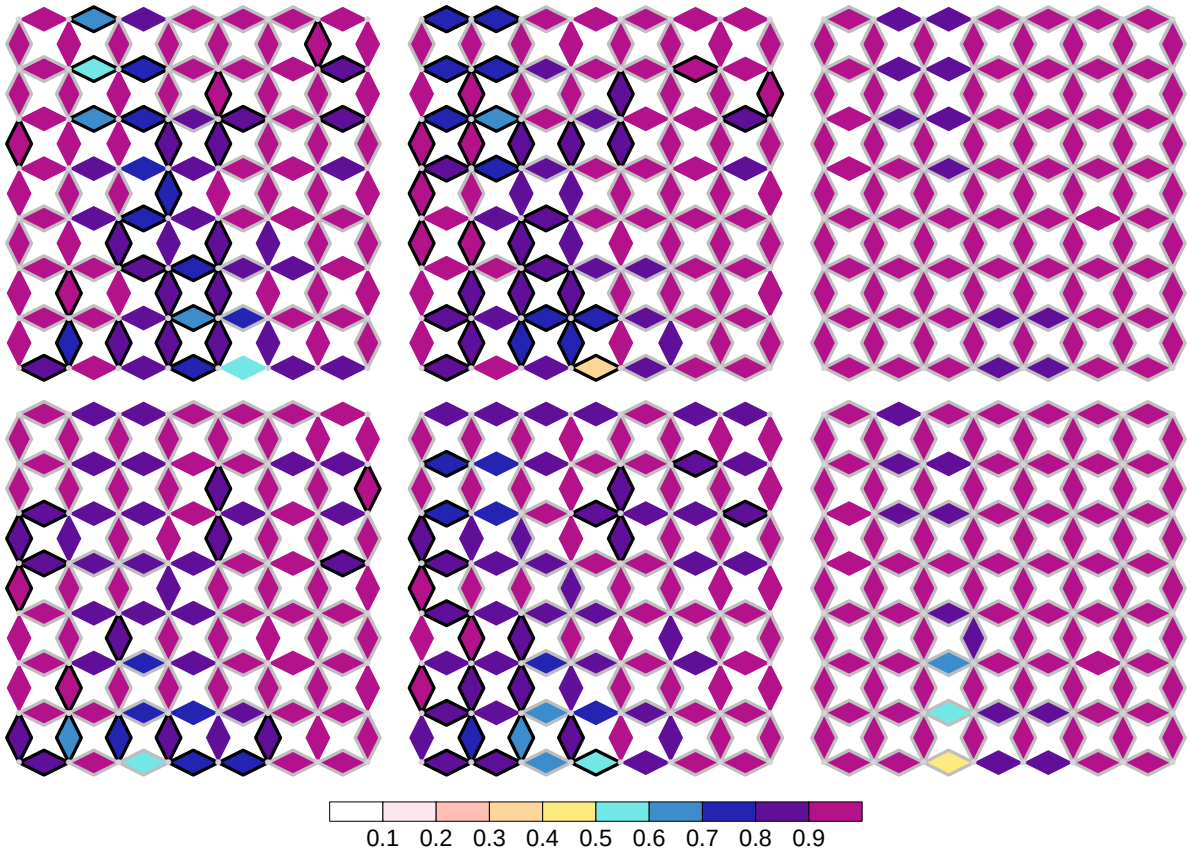

Figure S5. Rank correlation for neighbouring grid box pairs. Shown for DMI-HIRHAM5 (left), ETHZ-CLM (centre) and KNMI-RACMO2 (right) for winter (top) and summer (bottom) seasons. Grey dots: positions of underlying grid box centers; colour: strength of correlation. Black (grey) diamond borders for RCMs indicate a correlation significantly lower (higher) than for observations.

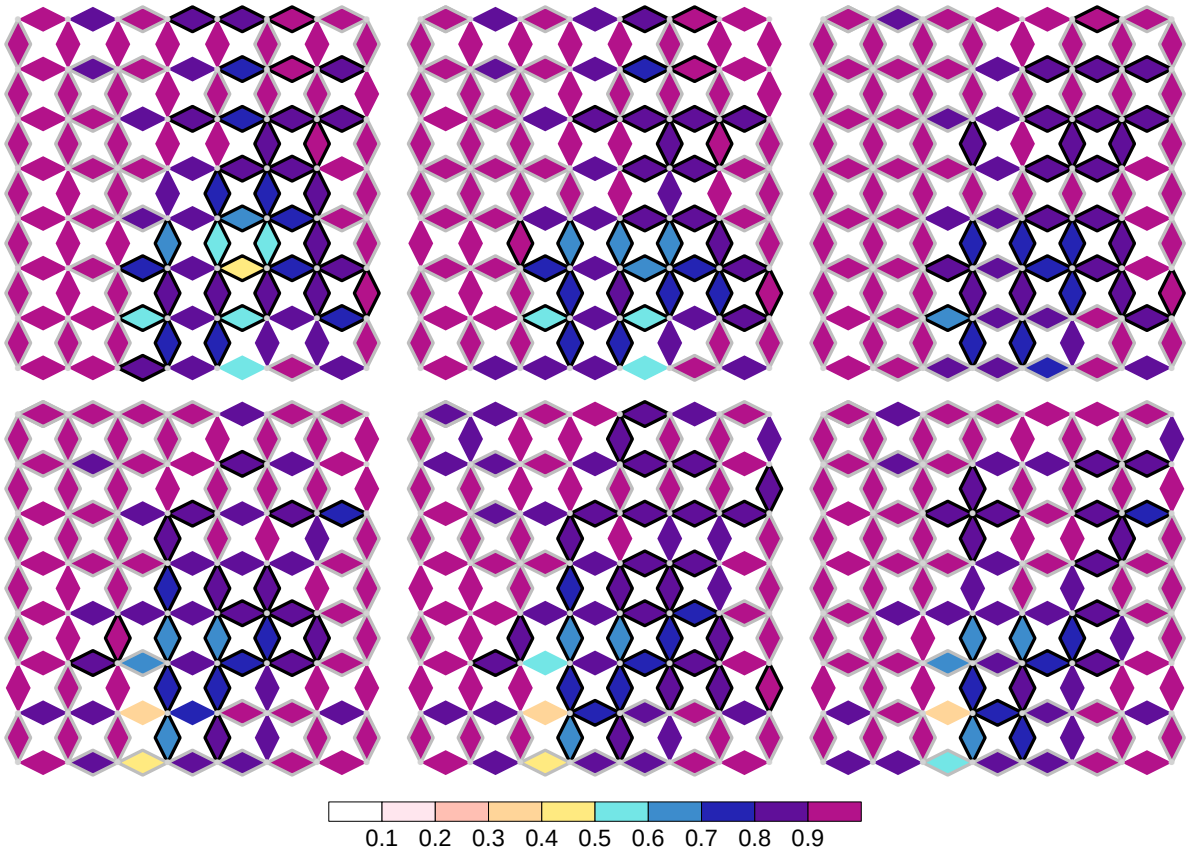

Figure S6. Rank correlation for neighbouring grid box pairs. Shown for METO-HC_HadRM3Q0 (left), METO-HC_HadRM3Q16 (centre) and METO-HC_HadRM3Q3 (right) for winter (top) and summer (bottom) seasons. Grey dots: positions of underlying grid box centers; colour: strength of correlation. Black (grey) diamond borders for RCMs indicate a correlation significantly lower (higher) than for observations.

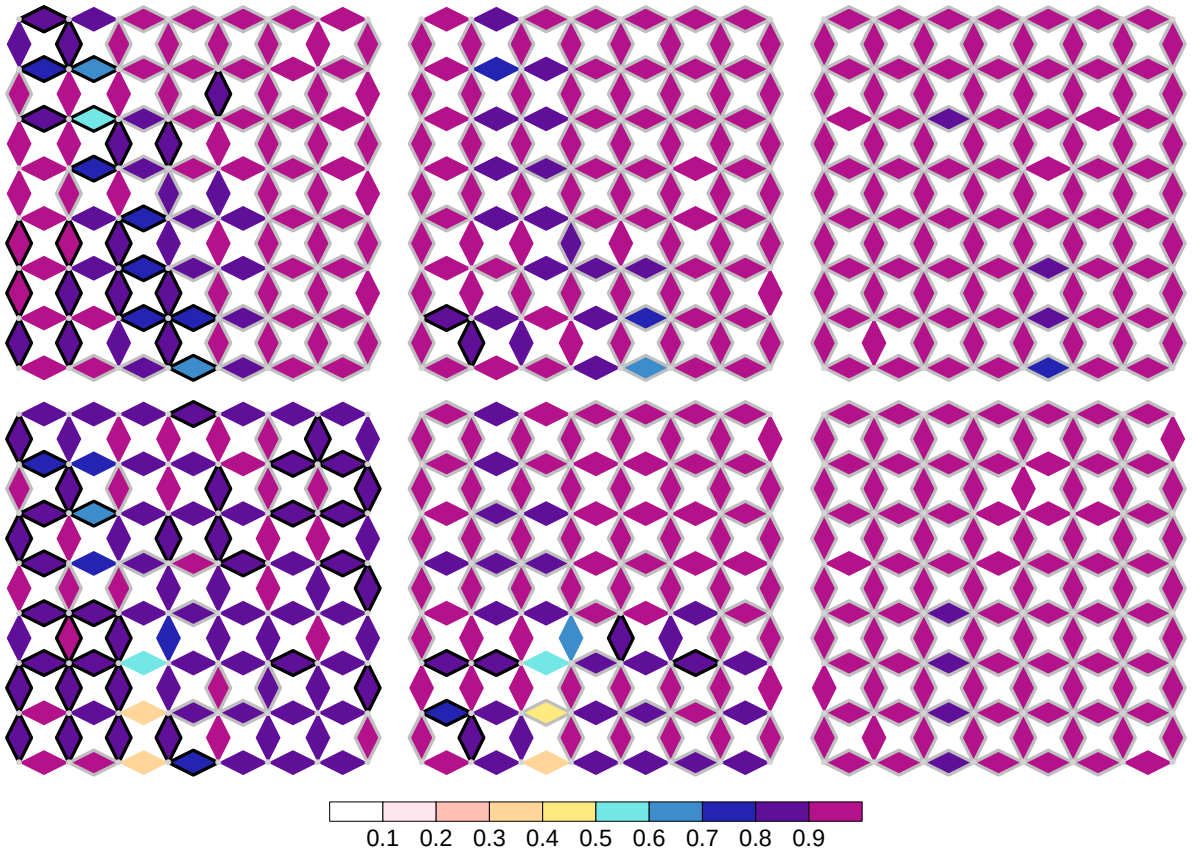

Figure S7. Rank correlation for neighbouring grid box pairs. Shown for MPI-M-REMO (left), RPN_GEMLAM (centre) and SMHIRCA (right) for winter (top) and summer (bottom) seasons. Grey dots: positions of underlying grid box centers; colour: strength of correlation. Black (grey) diamond borders for RCMs indicate a correlation significantly lower (higher) than for observations.

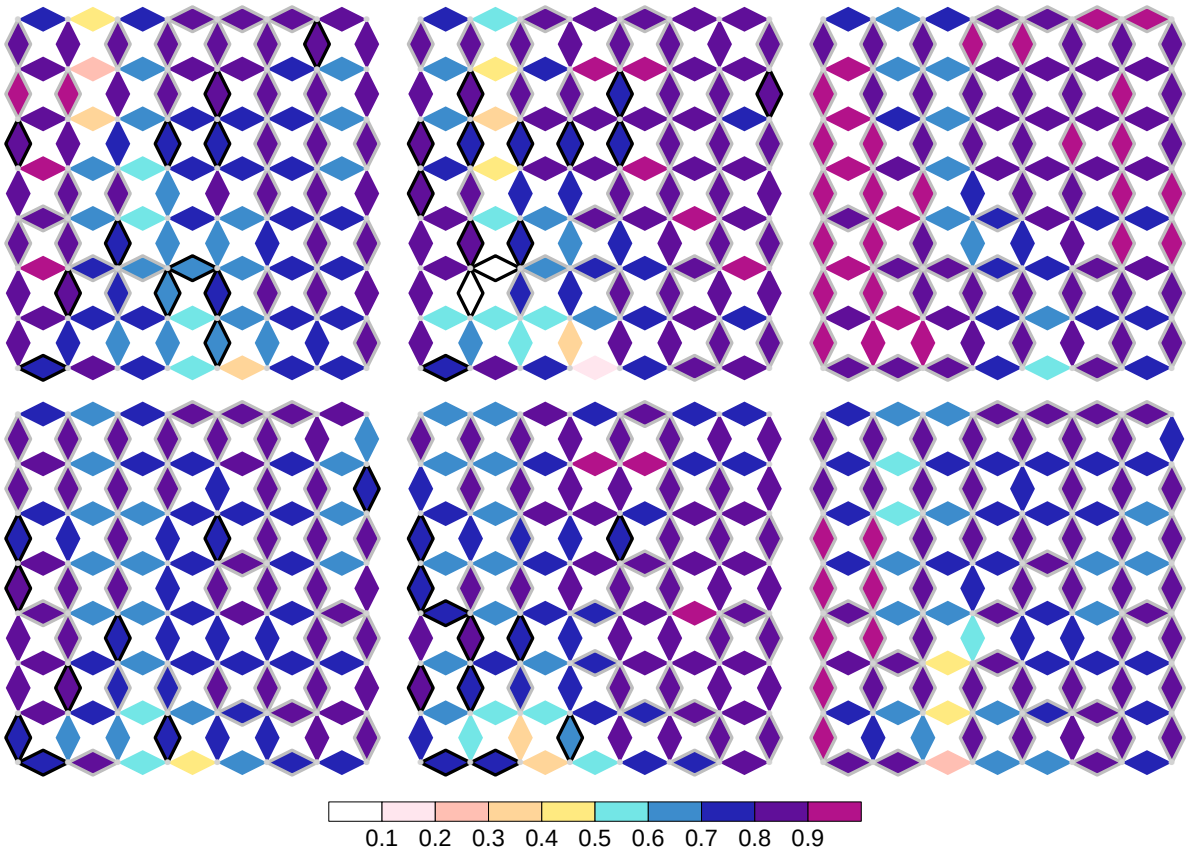

Figure S8. Upper tail dependence for neighbouring grid box pairs. Shown for DMI-HIRHAM5 (left), ETHZ-CLM (centre) and KNMI-RACMO2 (right) for winter (top) and summer (bottom) seasons. Grey dots: positions of underlying grid box centers; colour: strength of tail dependence. Black (grey) diamond borders for RCMs indicate a tail dependence significantly lower (higher) than for observations.

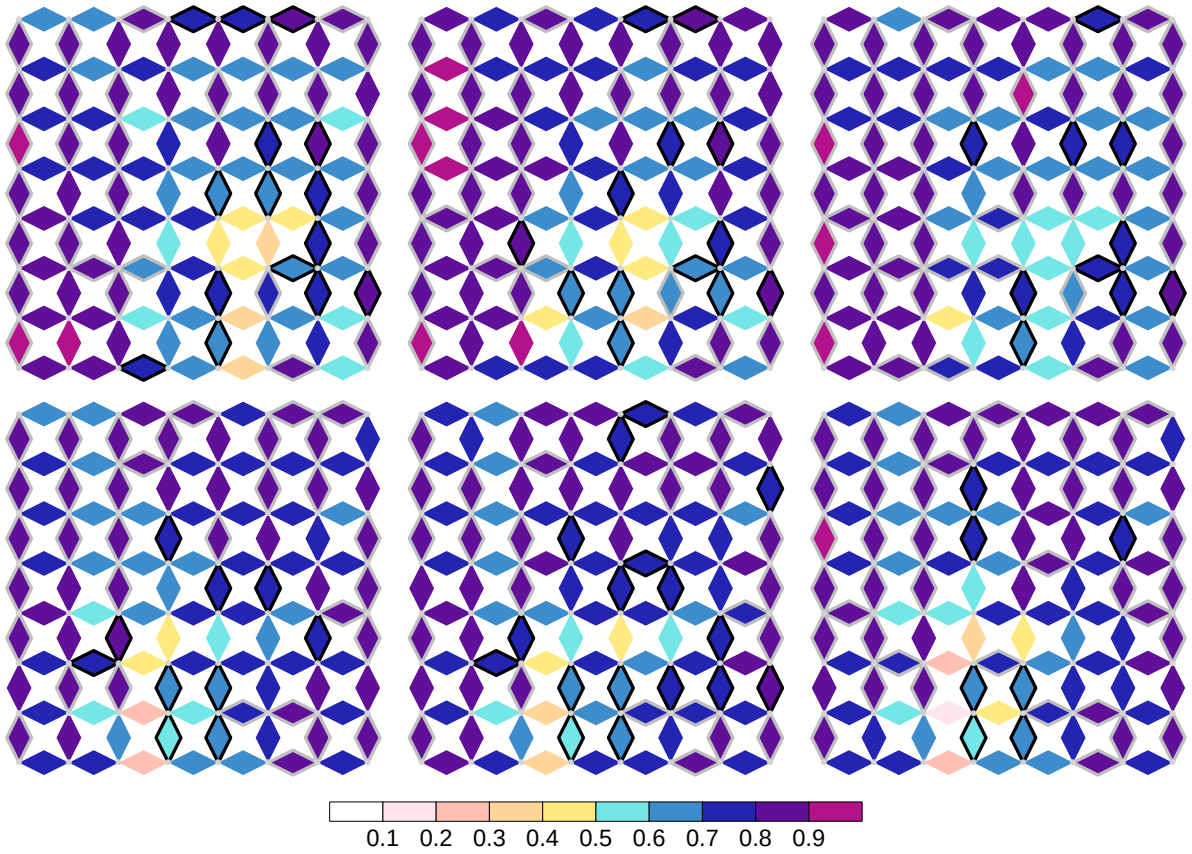

Figure S9. Upper tail dependence for neighbouring grid box pairs. Shown for METO-HC_HadRM3Q0 (left), METO-HC_HadRM3Q16 (centre) and METO-HC_HadRM3Q3 (right) for winter (top) and summer (bottom) seasons. Grey dots: positions of underlying grid box centers; colour: strength of tail dependence. Black (grey) diamond borders for RCMs indicate a tail dependence significantly lower (higher) than for observations.

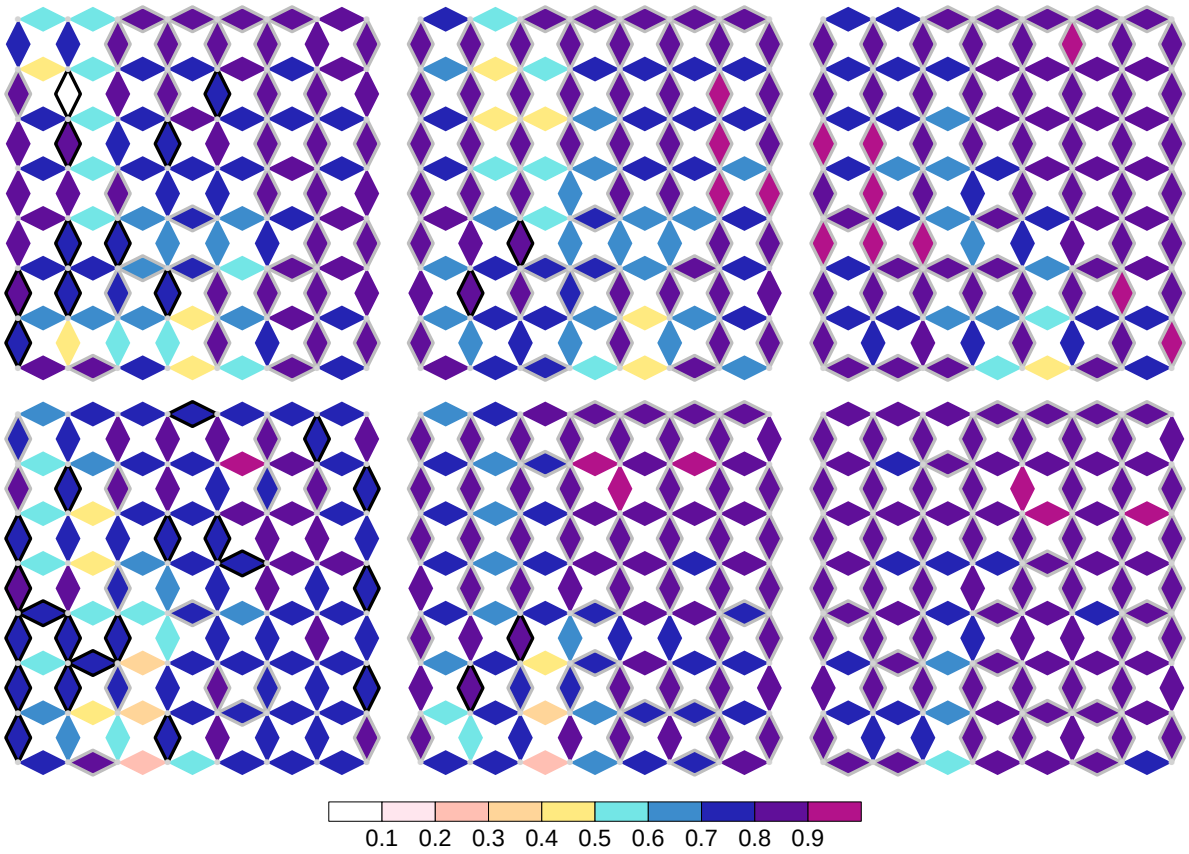

Figure S10. Upper tail dependence for neighbouring grid box pairs. Shown for MPI-M-REMO (left), RPN_GEMLAM (centre) and SMHIRCA (right) for winter (top) and summer (bottom) seasons. Grey dots: positions of underlying grid box centers; colour: strength of tail dependence. Black (grey) diamond borders for RCMs indicate a tail dependence significantly lower (higher) than for observations.

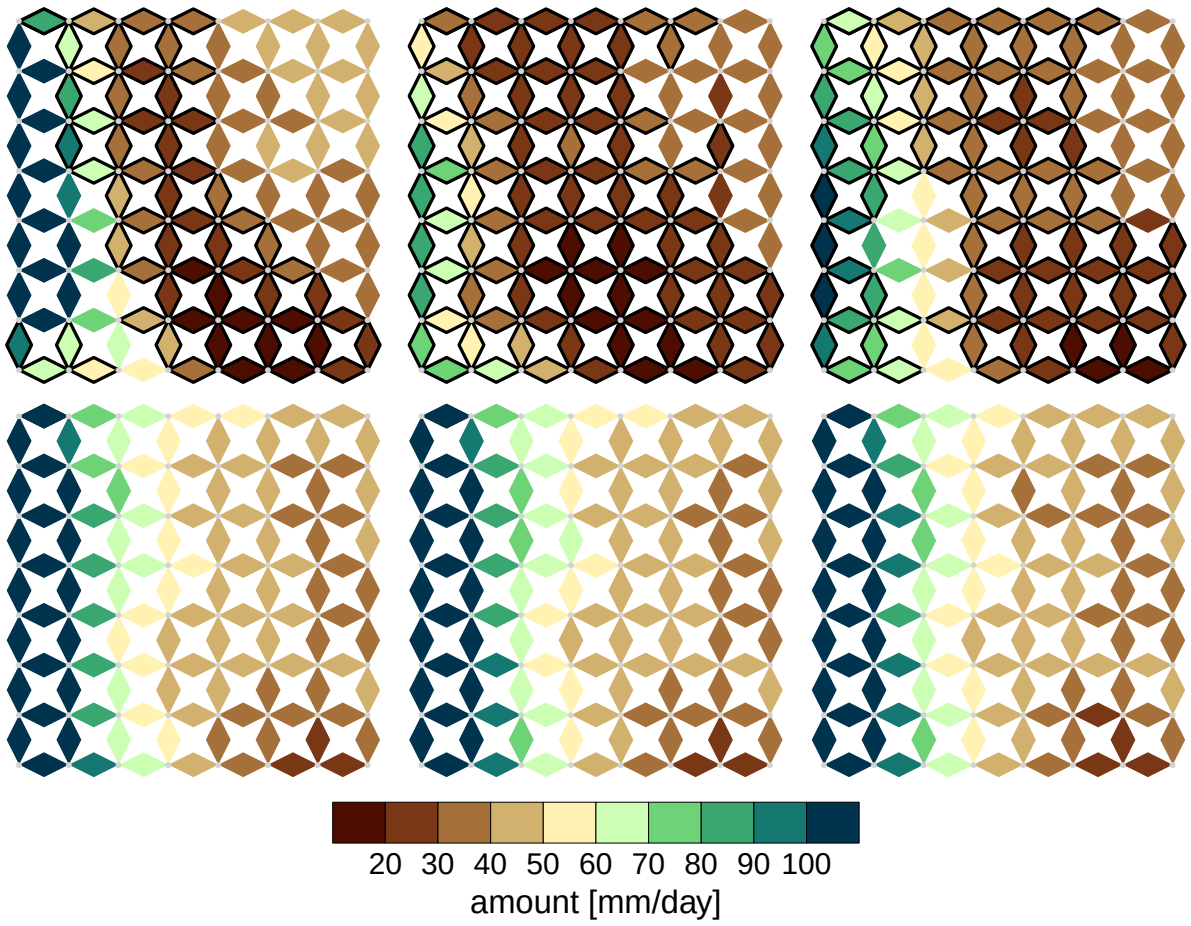

Figure S11. Area aggregated 95% quantiles of daily winter precipitation. Shown are DMI-HIRHAM5 (left), ETHZ-CLM (centre) and KNMI-RACMO2 (right). Top row: RCM margins and dependence (black (grey) diamonds: significantly lower (higher) than observations); bottom row: observed margins and RCM dependence (see text for details).

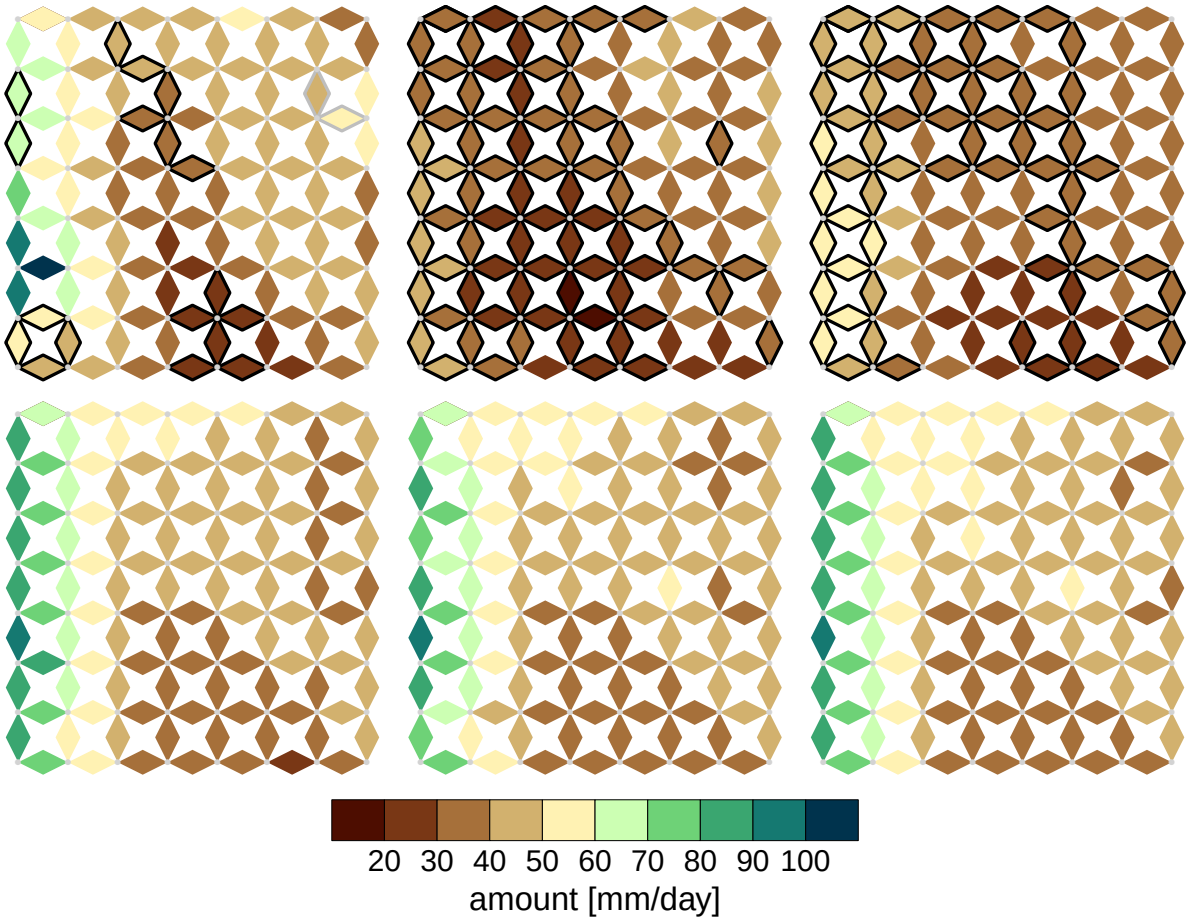

Figure S12. As Figure S11, but for summer.

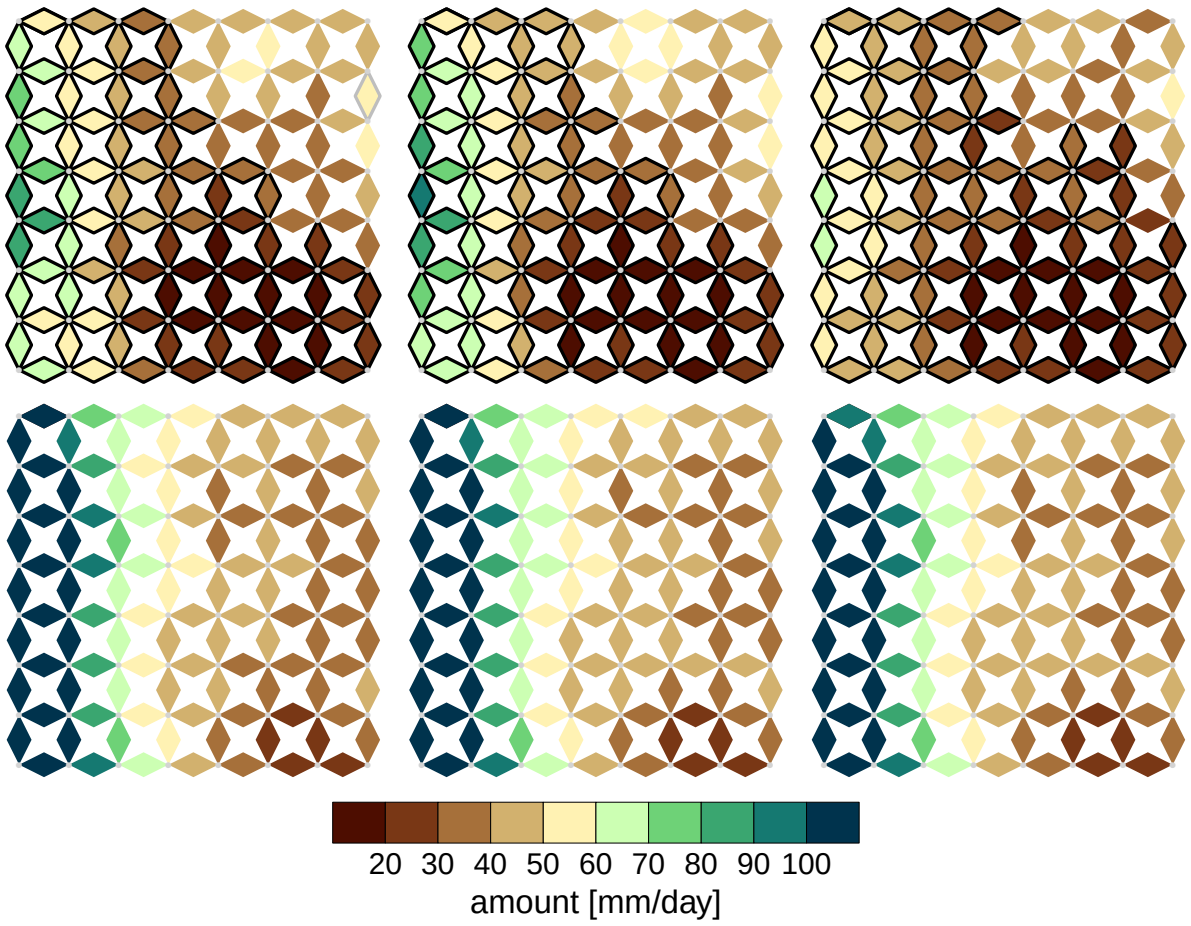

Figure S13. Area aggregated 95% quantiles of daily winter precipitation. Shown are METO-HC_HadRM3Q0 (left), METO-HC_HadRM3Q16 (centre) and METO-HC_HadRM3Q3 (right). Top row: RCM margins and dependence (black (grey) diamonds: significantly lower (higher) than observations); bottom row: observed margins and RCM dependence (see text for details).

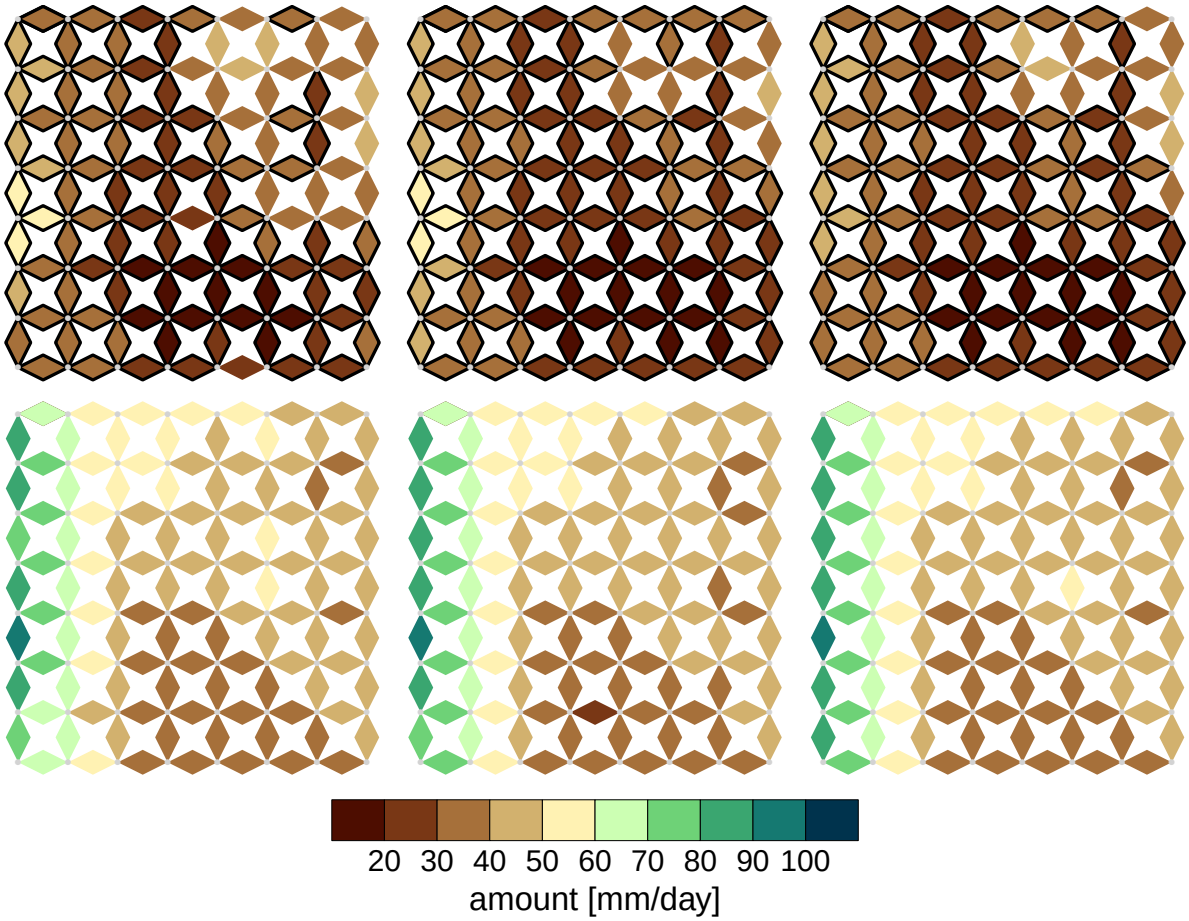

Figure S14. As Figure S13, but for summer.

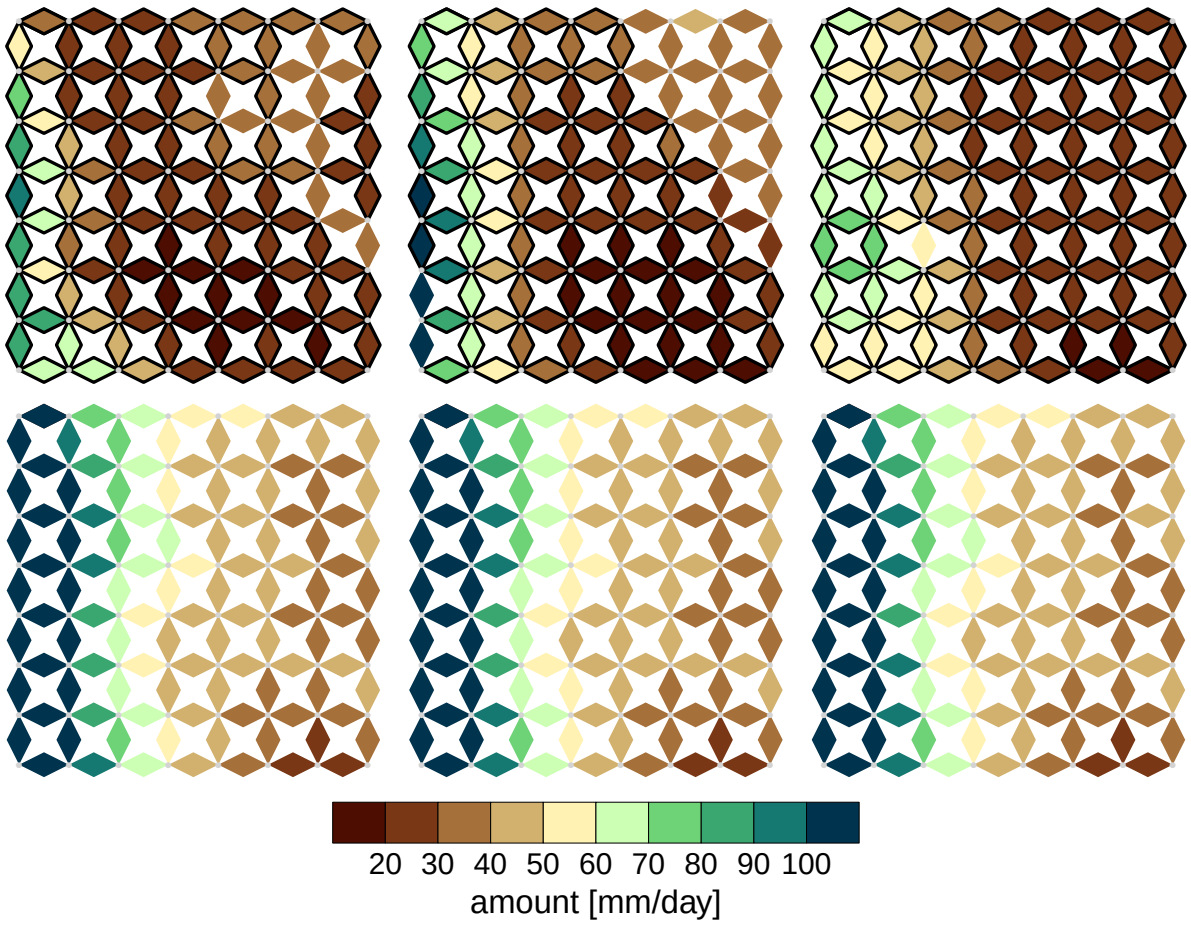

Figure S15. Area aggregated 95% quantiles of daily winter precipitation. Shown are MPI-M-REMO (left), RPN_GEMLAM (centre) and SMHIRCA (right). Top row: RCM margins and dependence (black (grey) diamonds: significantly lower (higher) than observations); bottom row: observed margins and RCM dependence (see text for details).

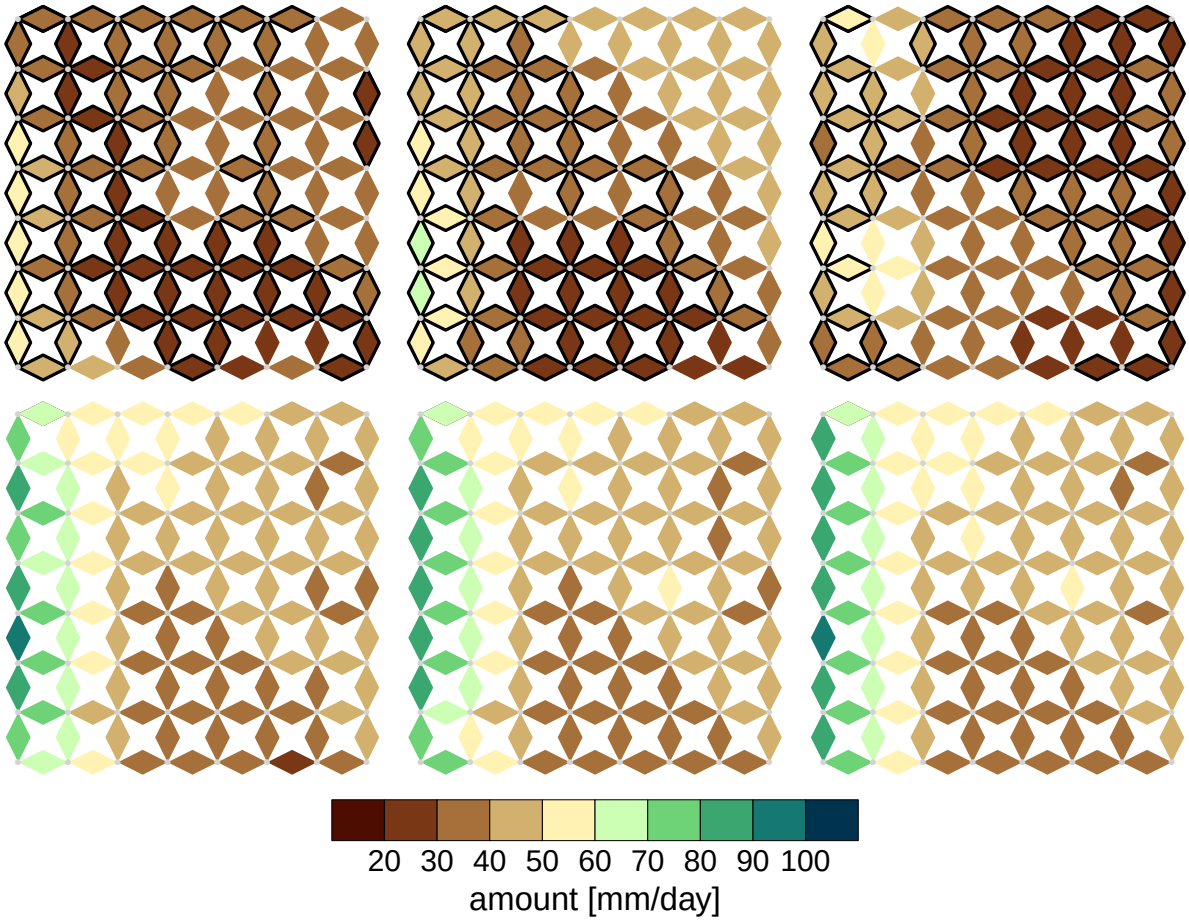

Figure S16. As Figure S15, but for summer.

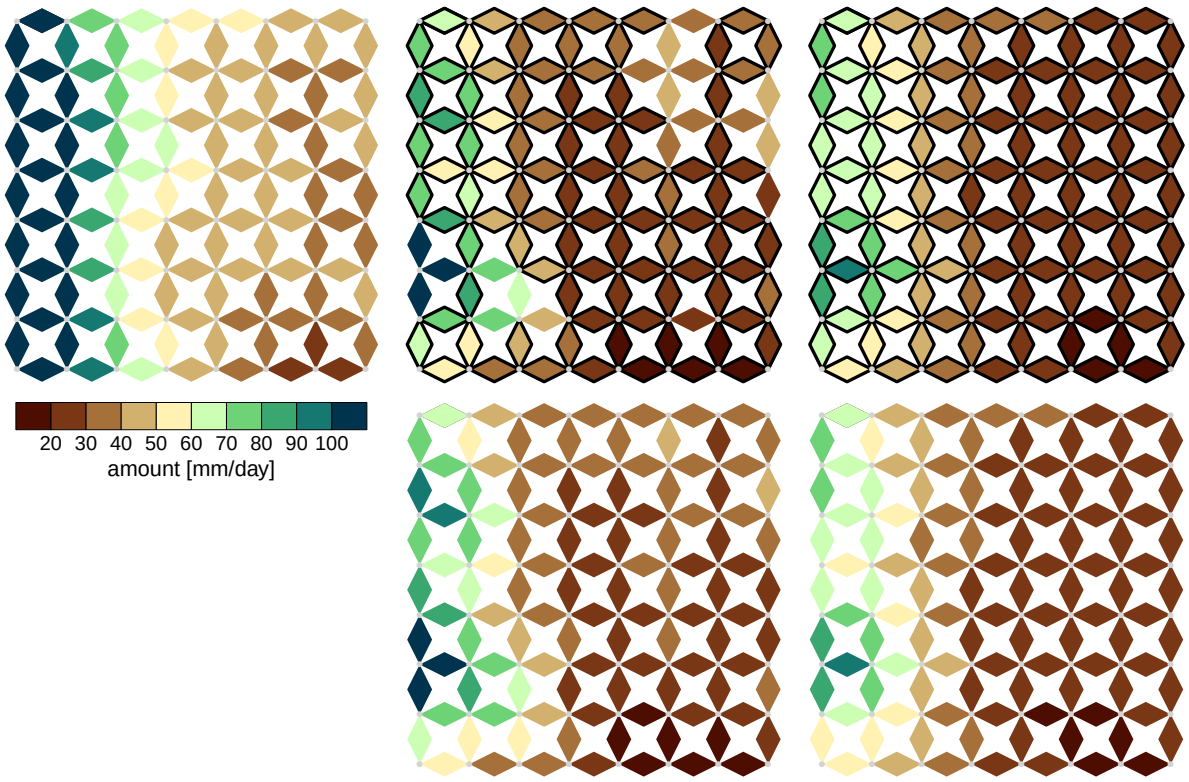

Figure S17. Area aggregated 95% quantiles of daily winter precipitation. Shown are observations (left), METNO-HIRHAM (centre) and C4IRCA3 (right). For models, top row: RCM margins and dependence (black (grey) diamonds: significantly lower (higher) than observations); bottom row: RCM margins and observed dependence (see text for details).

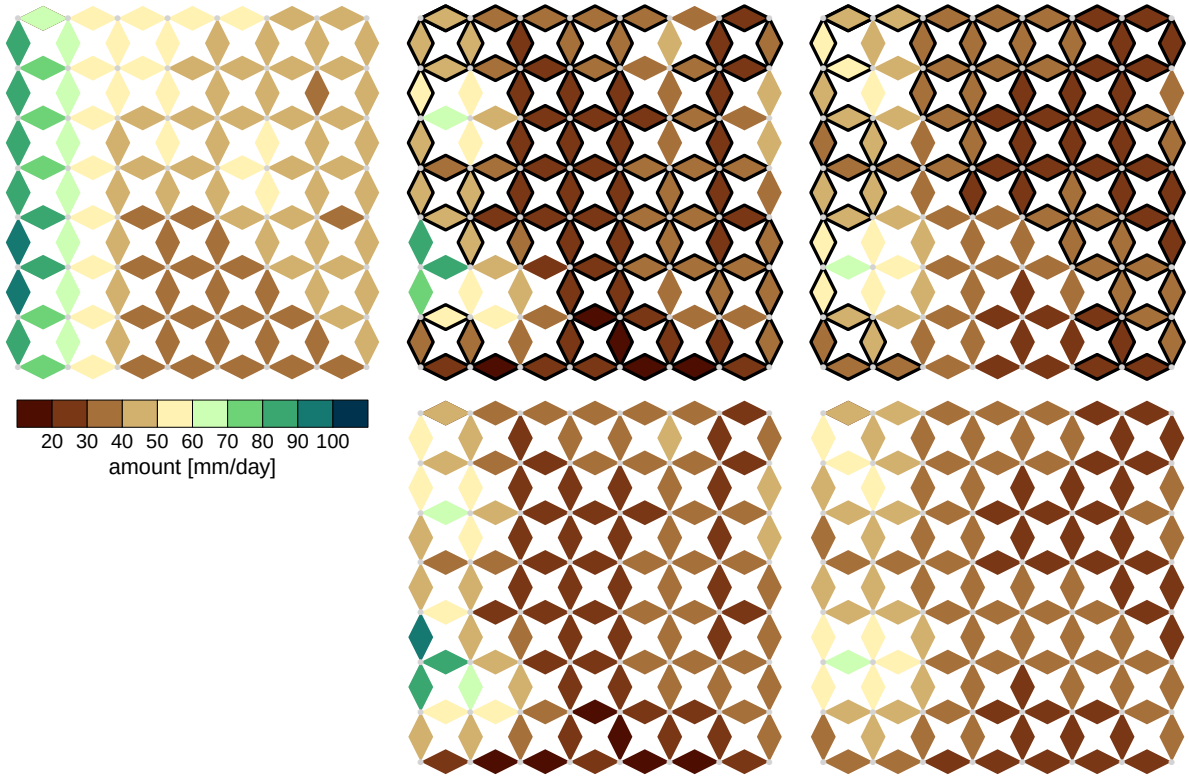

Figure S18. As Figure S17, but for summer.

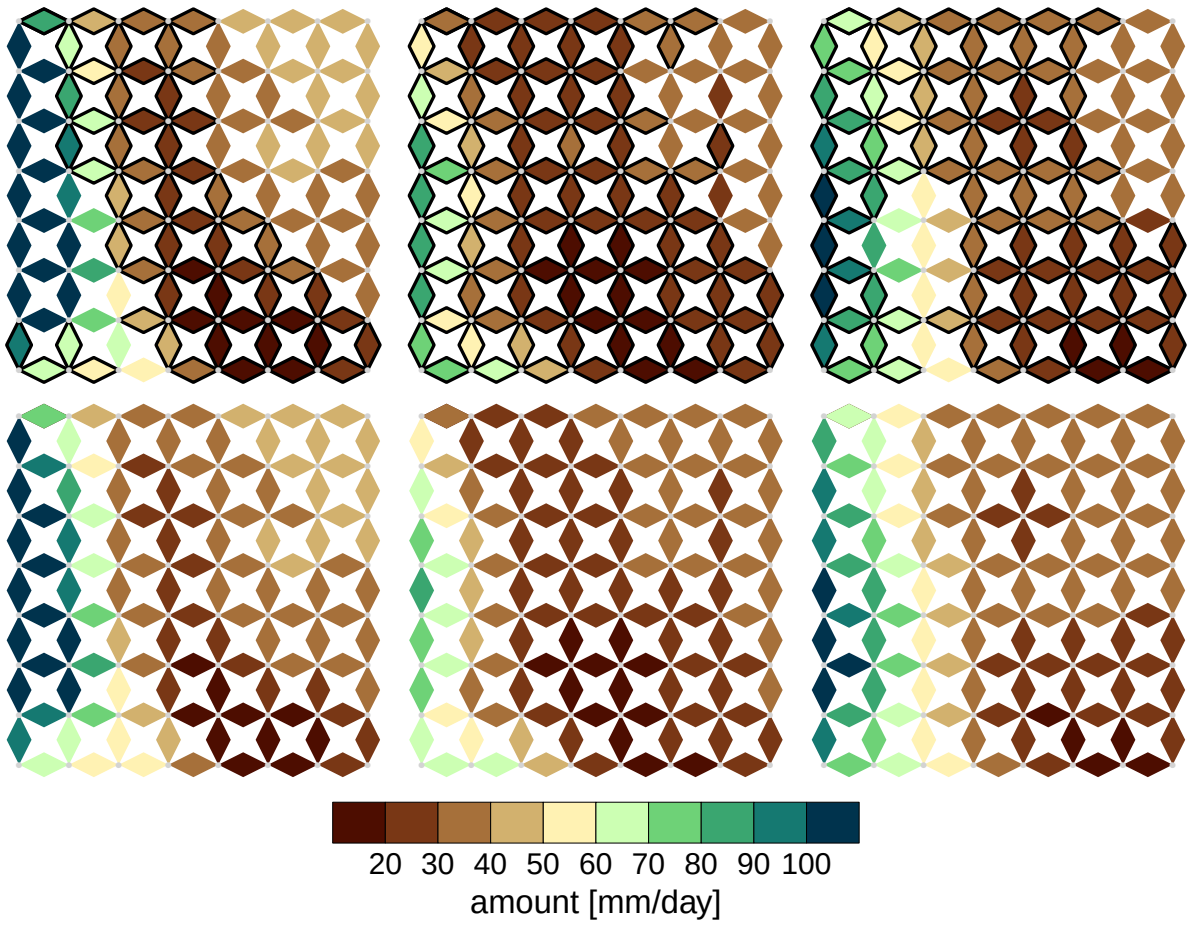

Figure S19. Area aggregated 95% quantiles of daily winter precipitation. Shown are DMI-HIRHAM5 (left), ETHZ-CLM (centre) and KNMI-RACMO2 (right). Top row: RCM margins and dependence (black (grey) diamonds: significantly lower (higher) than observations); bottom row: RCM margins and observed dependence (see text for details).

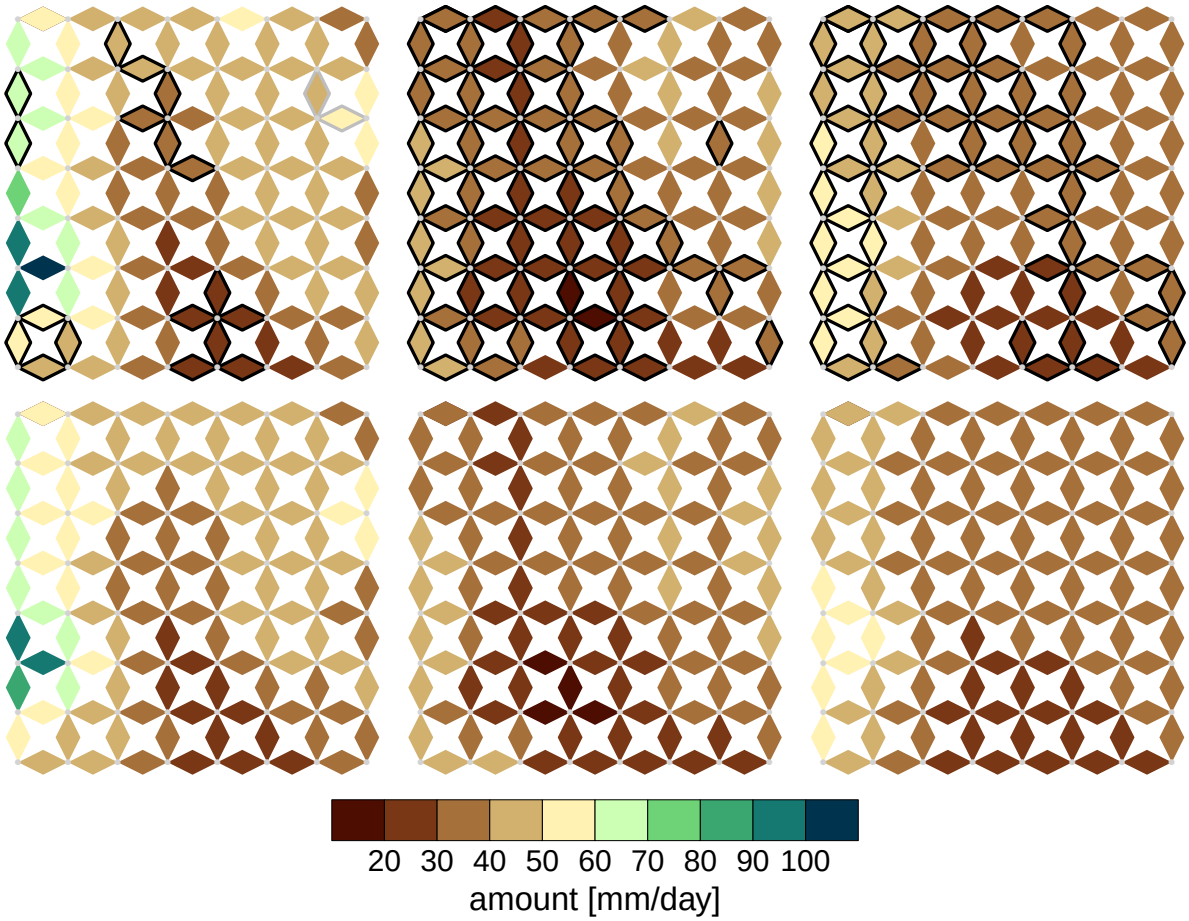

Figure S20. As Figure S19, but for summer.

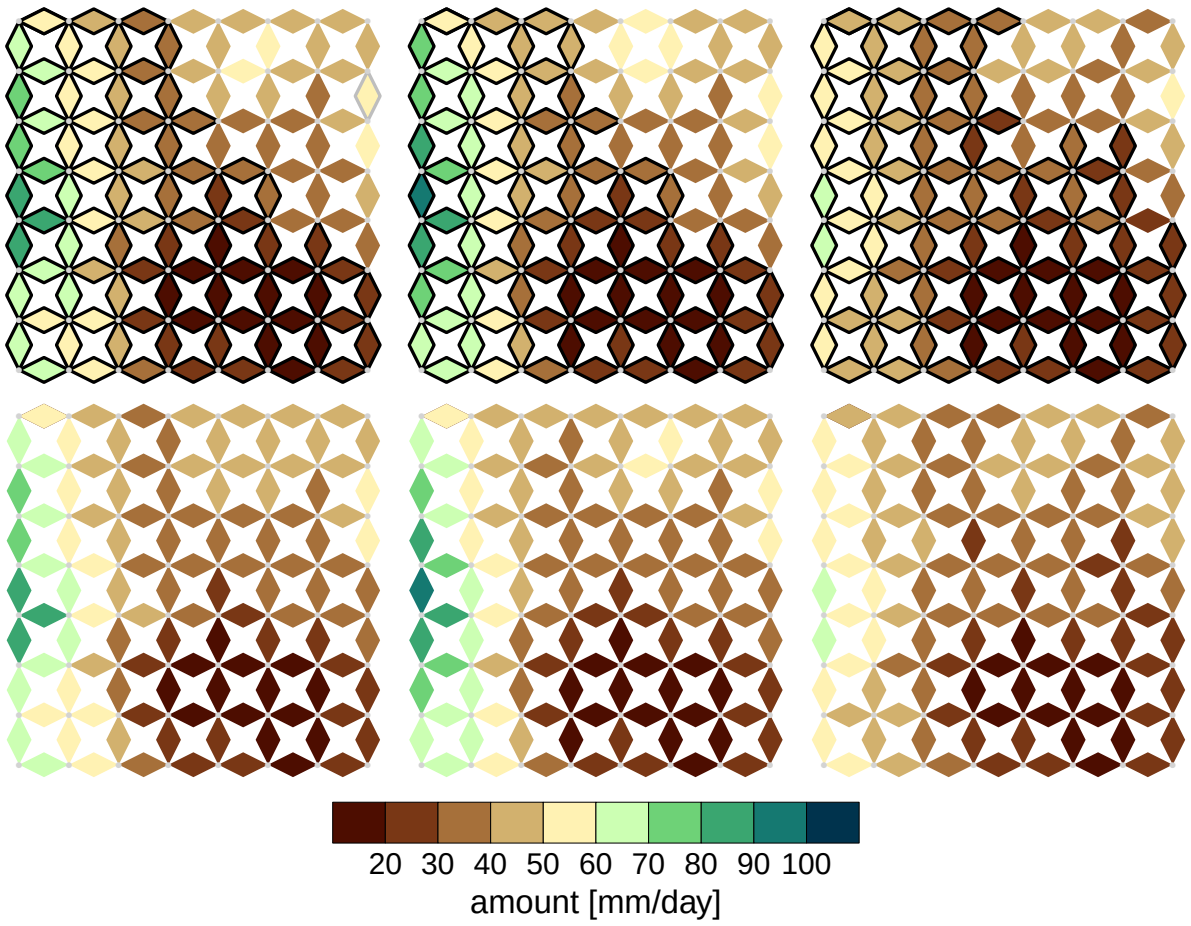

Figure S21. Area aggregated 95% quantiles of daily winter precipitation. Shown are METO-HC_HadRM3Q0 (left), METO-HC_HadRM3Q16 (centre) and METO-HC_HadRM3Q3 (right). Top row: RCM margins and dependence (black (grey) diamonds: significantly lower (higher) than observations); bottom row: RCM margins and observed dependence (see text for details).

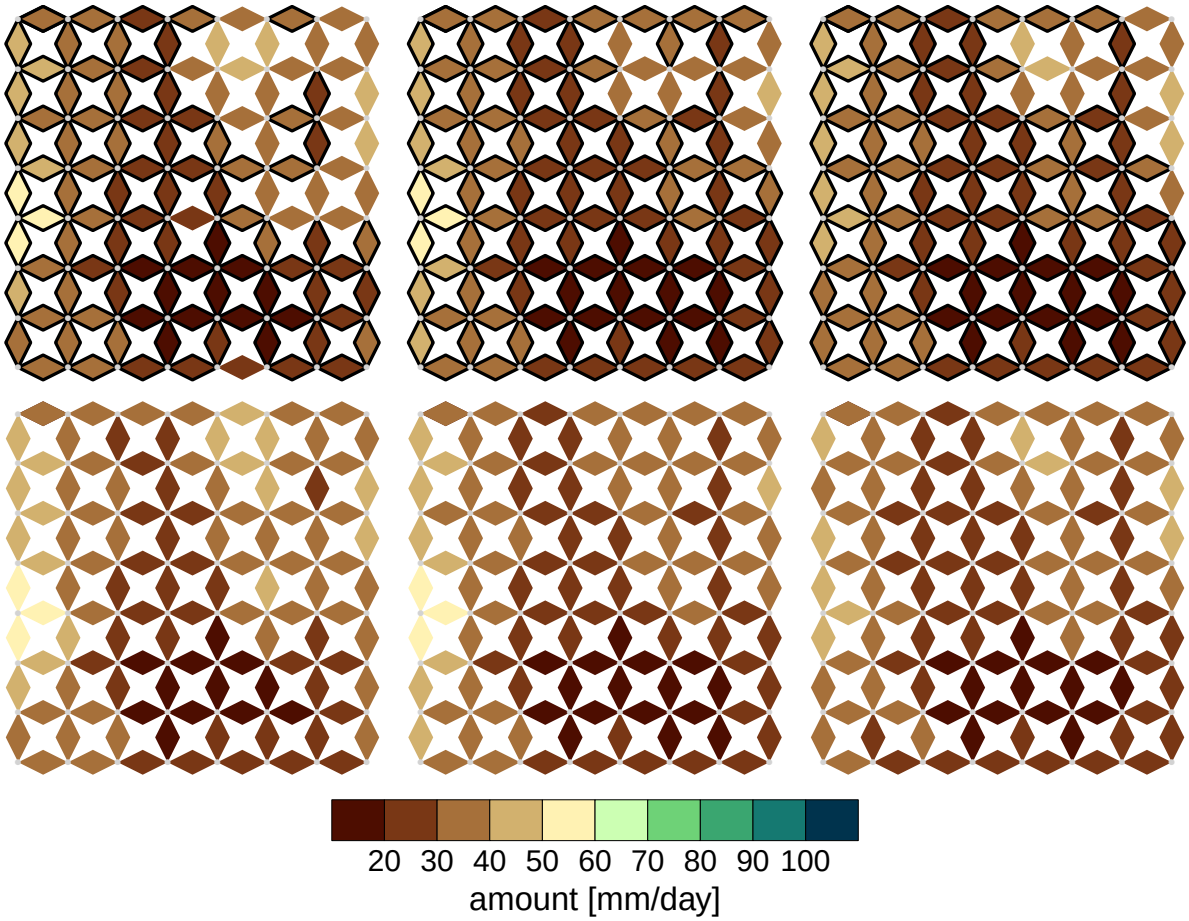

Figure S22. As Figure S21, but for summer.

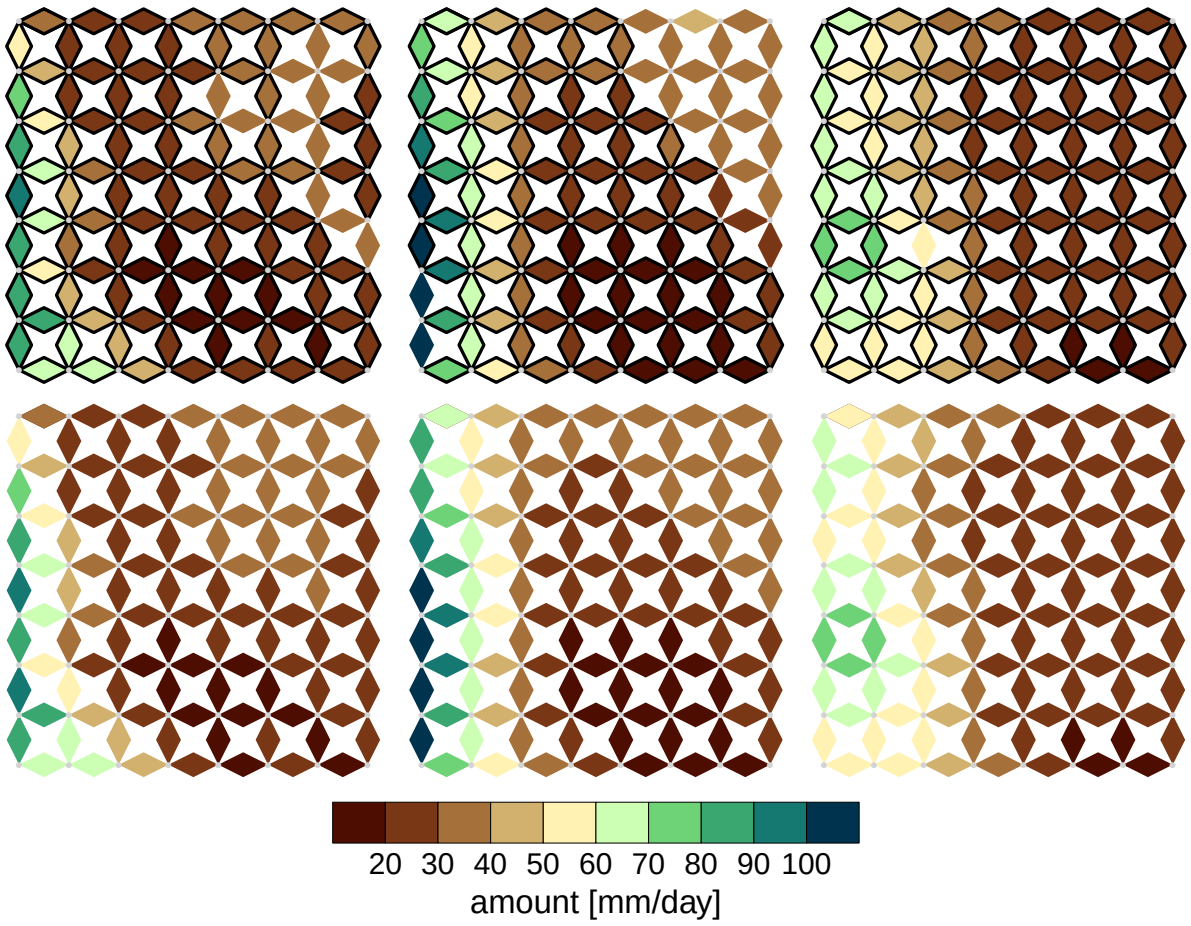

Figure S23. Area aggregated 95% quantiles of daily winter precipitation. Shown are MPI-M-REMO (left), RPN_GEMLAM (centre) and SMHIRCA (right). Top row: RCM margins and dependence (black (grey) diamonds: significantly lower (higher) than observations); bottom row: RCM margins and observed dependence (see text for details).

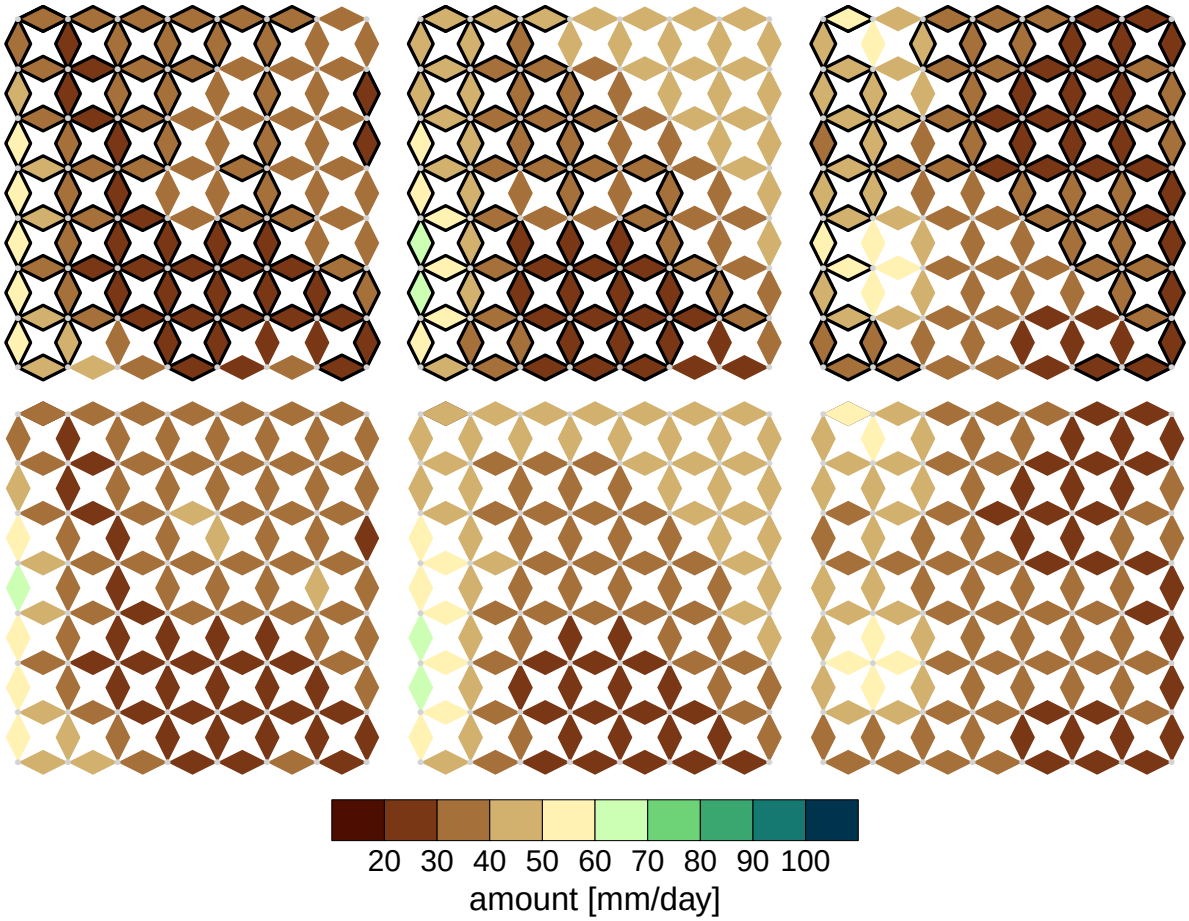

Figure S24. As Figure S23, but for summer.

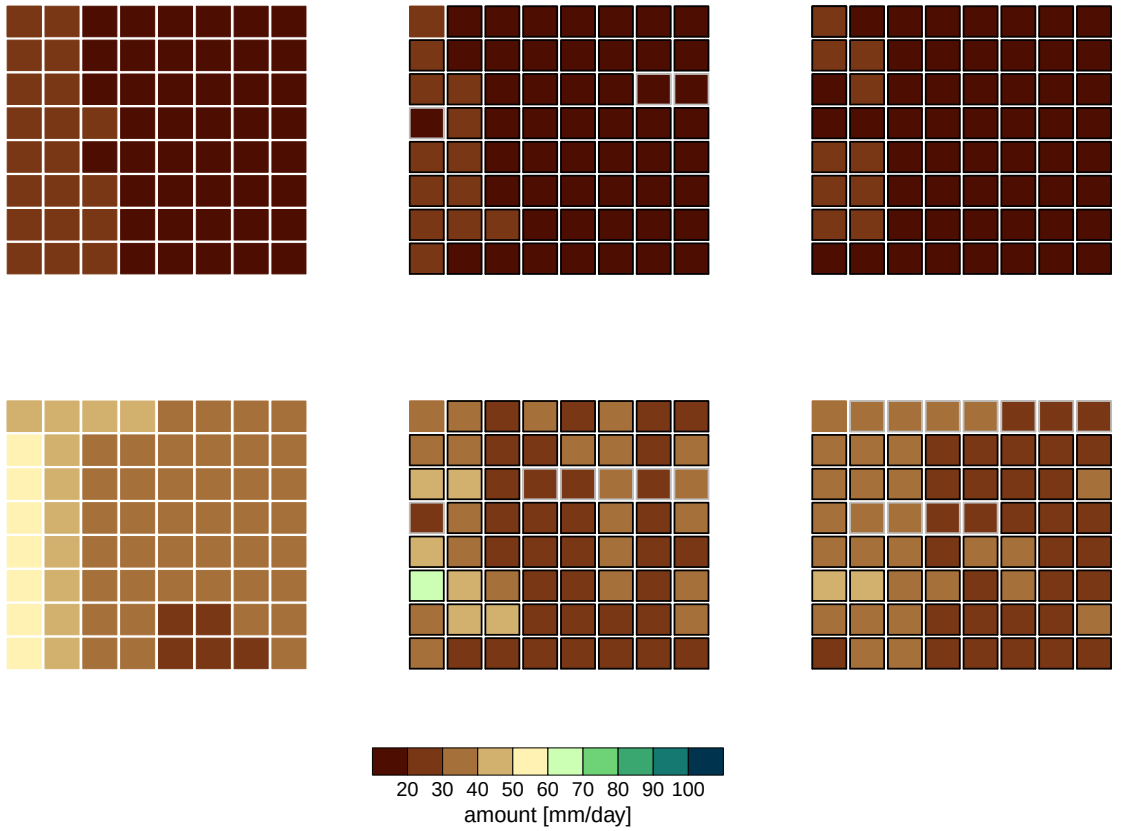

Figure S25. 95% quantiles of daily precipitation in each grid box from the winter (top) and summer (bottom) seasons. Shown are observations (left), METNO-HIRHAM (centre) and C4IRCA3 (right). Colour: magnitude of quantile. Black (grey) diamond borders for RCMs indicate a quantile significantly lower (higher) than for observations.

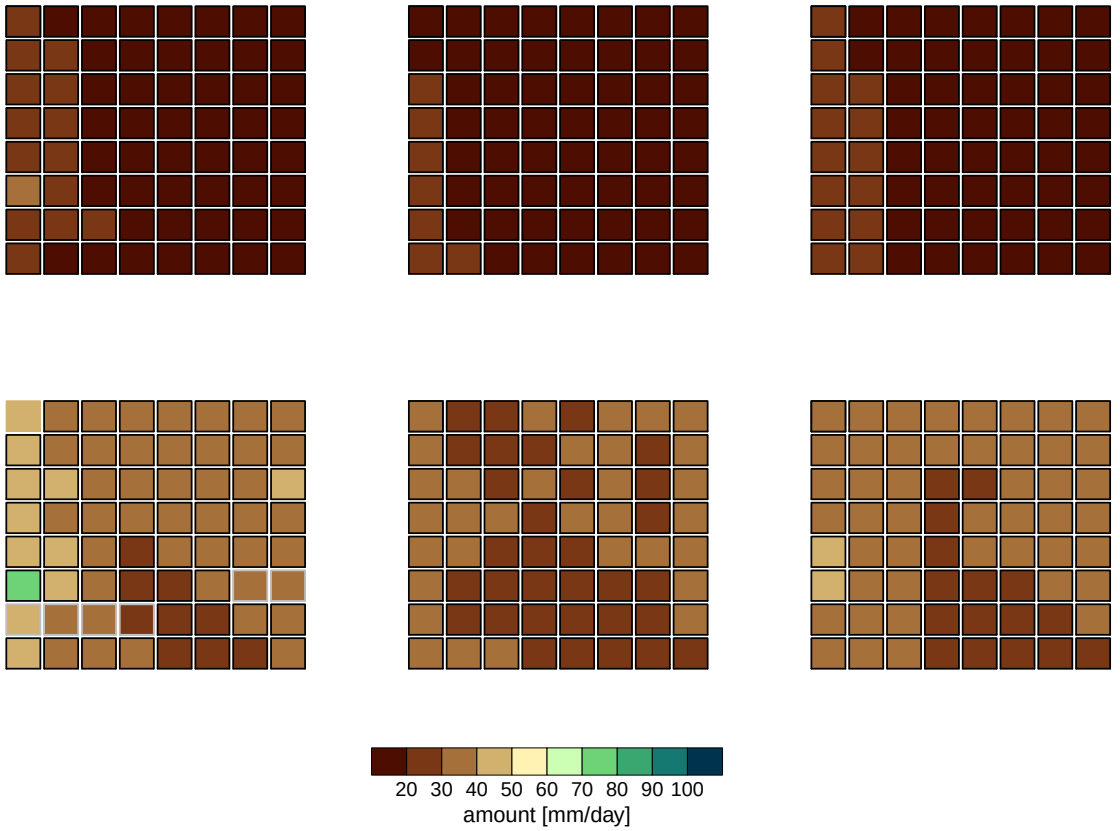

Figure S26. 95% quantiles of daily precipitation in each grid box from the winter (top) and summer (bottom) seasons. Shown are DMI-HIRHAM5 (left), ETHZ-CLM (centre) and KNMI-RACMO2 (right). Colour: magnitude of quantile. Black (grey) diamond borders indicate a quantile significantly lower (higher) than for observations.

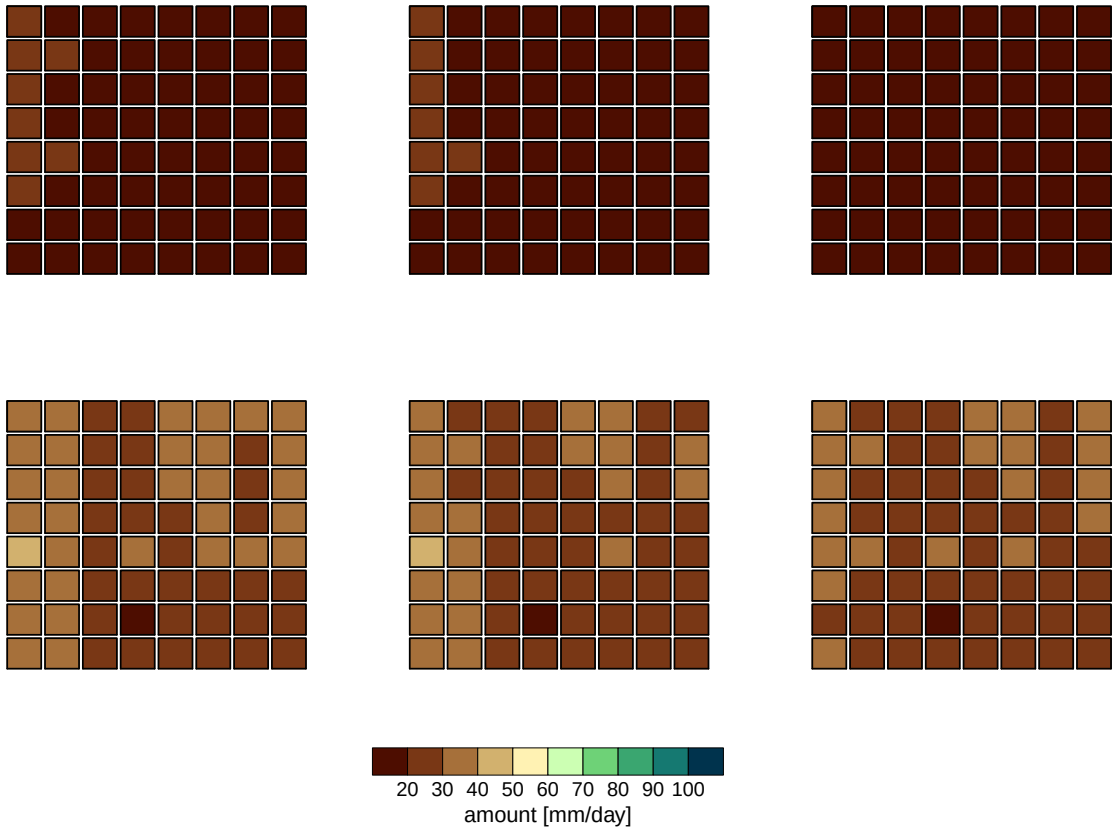

Figure S27. 95% quantiles of daily precipitation in each grid box from the winter (top) and summer (bottom) seasons. Shown are METO-HC_HadRM3Q0 (left), METO-HC_HadRM3Q16 (centre) and METO-HC_HadRM3Q3 (right). Colour: magnitude of quantile. Black (grey) diamond borders indicate a quantile significantly lower (higher) than for observations.

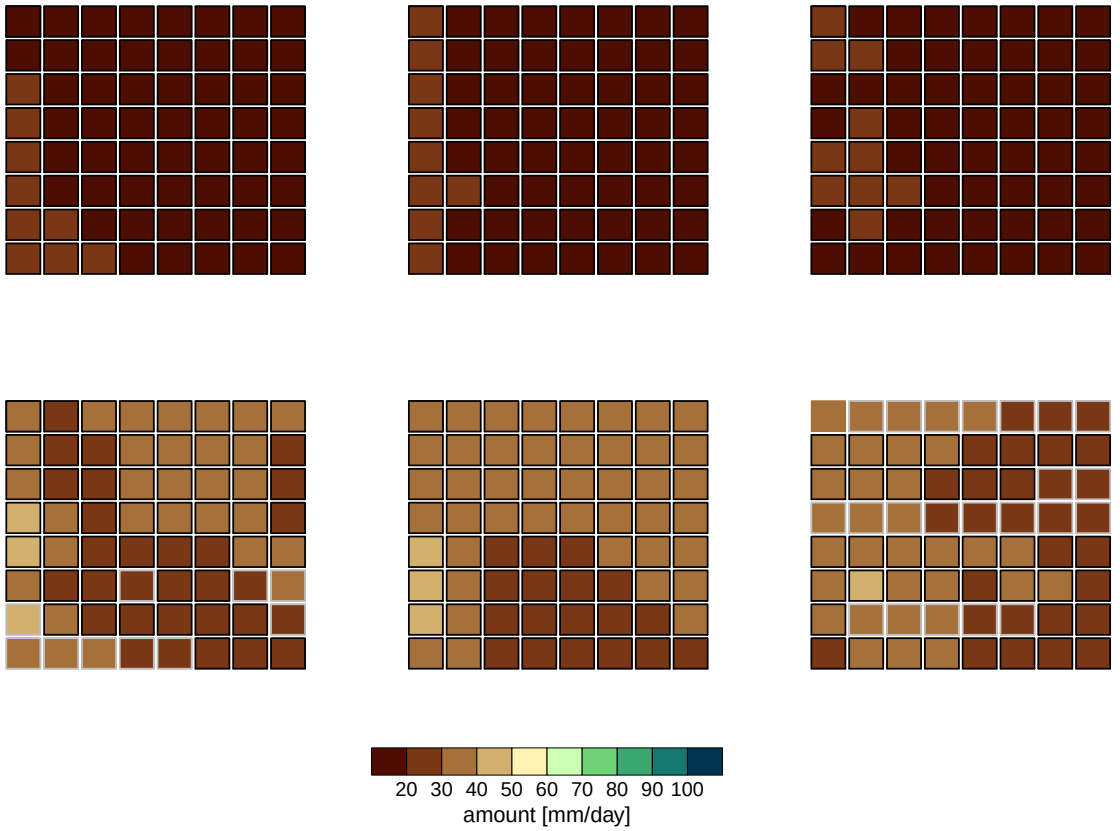

Figure S28. 95% quantiles of daily precipitation in each grid box from the winter (top) and summer (bottom) seasons. Shown are MPI-M-REMO (left), RPN_GEMLAM (centre) and SMHIRCA (right). Colour: magnitude of quantile. Black (grey) diamond borders indicate a quantile significantly lower (higher) than for observations.

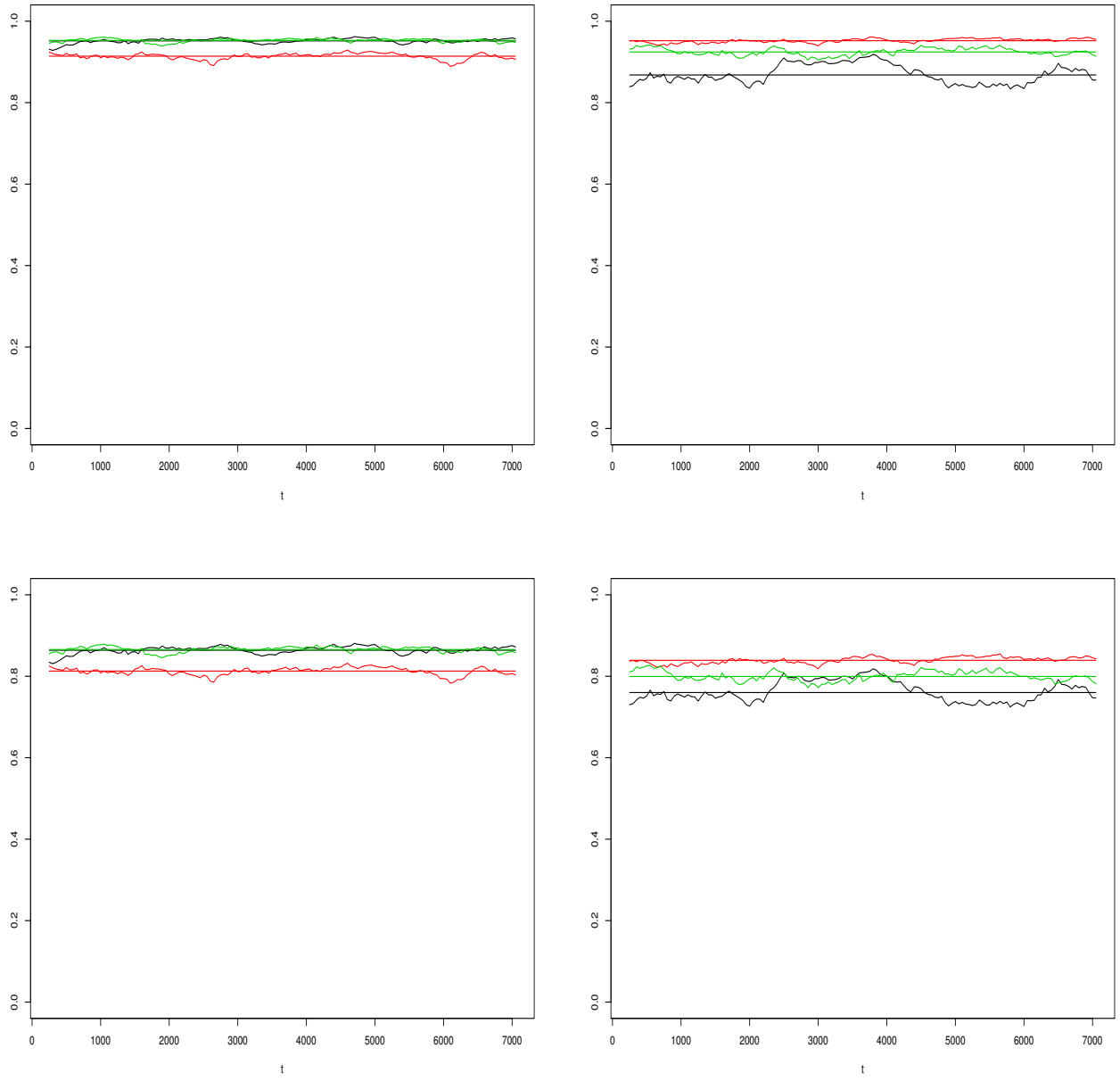

Figure S29. Spearman's ρ (upper row) and tail dependence between two cells (25 and 33 to the left and 42 and 43 to the right) for the winter season (black=observations, red=METNO-HIRHAM, green=DMI-HIRHAM5).

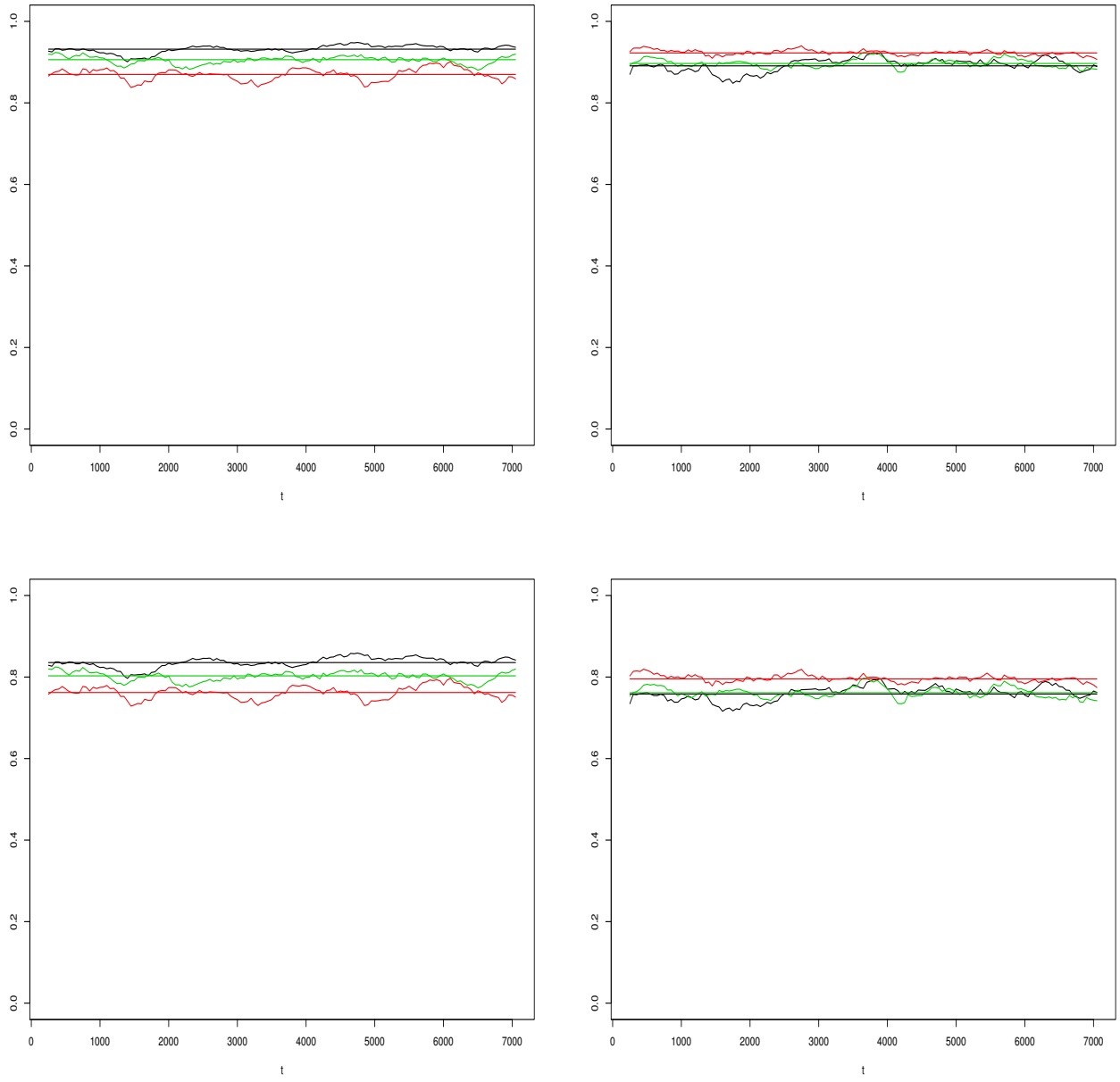

Figure S30. As Figure S29, but for summer.